PRAMANA
— journal of
physics

Vol. 73, No. 4
October 2009
pp. 657–668

Microscopic study of low-lying yrast spectra and deformation systematics in neutron-rich $^{98-106}$Sr isotopes

ANIL CHANDAN, SURAM SINGH, ARUN BHARTI* and S K KHOSA
Department of Physics, University of Jammu (J&K), Jammu 180 006, India
*Corresponding author. E-mail: arunbharti_2003@yahoo.co.in

MS received 15 January 2009; revised 7 May 2009; accepted 23 May 2009

Abstract. Variation-after-projection (VAP) calculations in conjunction with Hartree–Bogoliubov (HB) ansatz have been carried out for $A = 98$–106 strontium isotopes. In this framework, the yrast spectra with $J^{\Pi} \geq 10^{+}$, $B(E2)$ transition probabilities, quadrupole deformation parameter and occupation numbers for various shell model orbits have been obtained. The results of the calculation for yrast spectra give an indication that it is important to include the hexadecapole–hexadecapole component of the two-body interaction for obtaining various nuclear structure quantities in Sr isotopes. Besides this, it is also found that the simultaneous polarization of $p_{3/2}$ and $f_{5/2}$ proton subshells is a significant factor in making a sizeable contribution to the deformation in neutron-rich Sr isotopes.

Keywords. Nuclear structure of $^{98-106}$Sr; variation-after-projection (VAP) calculations; calculated levels; $B(E2)$ transition probabilities; quadupole β_2 deformation parameter.

PACS Nos 21.60.-n; 21.60.Jz; 27.60.+j

1. Introduction

The existence of a large deformation in the neutron-rich nuclei in the mass region $A = 100$ was established by Cheifetz *et al* [1]. Since then considerable effort has gone in understanding the properties of this region. It has been observed that neutron-rich isotopes with $N \geq 60$ and $A \approx 100$ are characterized by strong axial deformations. Quadrupole deformation of $\beta = 0.4$ has been deduced for ^{98}Sr and ^{100}Sr from the lifetimes of the first excited states and from mean square radii measured by collinear laser spectroscopy [2–6]. According to these results, ground state deformation remains constant after its sudden onset at $N = 60$. This trend even could continue at larger neutron numbers. The recent development in experimental techniques like the decay of on-line mass separated ^{98}Rb to ^{98}Sr by γ-spectroscopy [7] make attractive a compilation of some of the more general features of the structure of doubly even neutron-rich Sr isotopes. The ^{98}Sr nucleus is well deformed.

The ground state band of ^{98}Sr, in particular, exhibits excellent rotational properties with a large and rigid moment of inertia. ^{98}Sr is predicted to have a well-deformed prolate ground state. The levels in ^{100}Sr were first observed in a β-decay study of ^{100}Rb by Azuma *et al* [8] who identified the $4^+ \rightarrow 2^+ \rightarrow 0^+$ cascade and performed the first lifetime measurement of the 2^+ state, thereby, establishing large deformations. Further members of the ground state band upto $I^\pi = 10^+$ were identified in prompt-fission studies [9]. Sometime back, evidence for the 2^+ level in ^{102}Sr was observed from the decay study of ^{102}Rb mass separated at the CERN-ISOLDE Facility [10]. It has been recently predicted [11] that ^{102}Sr is a strongly deformed nucleus with properties close to the rotational limit. Presently, the ^{102}Sr nucleus is the most deformed neutron-rich even–even isotope in the Sr region.

From the systematics of the 2^+ states in neutron-rich Sr isotopes, one observes large decrease in E_2^+ energy as neutron number N changes from 58 to 60. The onset of deformation in this region for Sr is the most abrupt known for even–even nuclei, as evidenced by the fact that the 2^+ energy decreases by a factor of 5.7 as N increases from 58 to 60 [12]. Besides this, it is also observed that the energy of the 2^+ state decreases from 0.144 MeV in ^{98}Sr to 0.126 MeV in ^{102}Sr giving an indication that there is an increase in the degree of deformation as one moves from ^{98}Sr to ^{102}Sr. The experimental data for $^{104-106}$Sr are not available. From the observed data, it is clear that ^{102}Sr is the most deformed nucleus in the Sr region.

A microscopic explanation for the onset of deformation at $N = 60$ has been given by Federman and Pittel [13]. They argued that strong attractive n–p interaction between $(g_{7/2})\nu$ and $(g_{9/2})\pi$ spin-orbit partner (SOP) orbitals are the underlying cause of the unusual characteristics. The realization of large deformation requires that the spin-orbit partner orbitals lie near the Fermi surface, both prior to and after the onset of deformation. There is another school of thought put forth by mean-field theorists [14,15] who have assigned the development of large deformation in $A = 100$ region to the occupation of low k-components of $(h_{11/2})\nu$ orbit. They find their mean field calculations indicating the appearance of $k = 1/2$ component of $(h_{11/2})\nu$ orbit at the Fermi surface in $^{100-102}$Sr. It was shown by the authors in [16–19] that the phenomenological pairing plus quadrupole–quadrupole (PQ) model of the two-body interaction is highly reliable in this mass region. It was shown by Khosa and Sharma [19] that, two-body effective interactions have a dominantly quadrupole–quadrupole character and the deformation-producing tendency of neutron–proton (n–p) and like-particle interactions depend upon the degeneracy of the underlying single-particle valence space. One of the natural choices for the two-body residual interaction would, therefore, be pairing plus quadrupole–quadrupole (PQ). It turns out from the calculated values of energy spectra obtained with PQ interaction that, the agreement with experiment is not satisfactory. It becomes, therefore, necessary to add a correction term to the PQ interaction in the form of hexadecapole–hexdecapole interaction, which hereafter will be denoted as PQH interaction.

The purpose of the present work is to know whether the PQ model of two-body interaction can further be modified to produce better results in agreement with the experiments. We have, thus, examined the available yrast spectra in deformed neutron-rich Sr isotopes with $A = 98$–106 in the framework of variation-after-projection (VAP) technique in conjunction with the HB ansatz for the trial wave

functions resulting from PQH interaction. The deformed Hartree–Fock–Bogoliubov state of the nucleus is generated using a phenomenological PQH interaction with ^{56}Ni as the core.

The VAP prescription selects an optimum intrinsic state for each yrast level through a minimization of the expectation value of the Hamiltonian with respect to the states characterized by a definite angular momentum. Our VAP calculations performed with PQH model of two-body interaction show a marked improvement in agreement with the experimentally observed yrast spectra as compared to the yrast spectra obtained with the PQ interaction. The results obtained for $B(E2)$ transition probabilities and quadrupole deformation parameter (β_2) are also found to be in reasonably good agreement with the experiments.

2. Calculational details

2.1 *The one- and two-body parts of Hamiltonian*

In our calculations presented here, we have employed the valence space spanned by $3s_{1/2}$, $2p_{1/2}$, $2p_{3/2}$, $2d_{3/2}$, $2d_{5/2}$, $1f_{5/2}$, $1g_{7/2}$, $1g_{9/2}$ and $1h_{11/2}$ orbits for protons and neutrons under the assumption of $N = Z = 28$ subshell closure. The single-particle energies (SPEs) that we have taken are (in MeV): $(3s_{1/2}) = 9.90$, $(2p_{1/2}) = 1.08$, $(2p_{3/2}) = 0.0$, $(2d_{3/2}) = 11.40$, $(2d_{5/2}) = 8.90$, $(1f_{5/2}) = 0.78$ $(1g_{7/2}) = 11.90$, $(1g_{9/2}) = 3.50$ and $(1h_{11/2}) = 12.90$. The energy values of single-particle orbits for $2p$–$1f$–$1g$ levels is the same as employed for ^{56}Ni core plus one nucleon. The energies of higher single-particle valence orbits is the same as used by Vergados and Kuo [20] relative to $1g_{9/2}$ valence orbit.

The two-body effective interaction that has been employed is of PQH type. The parameters of PQ part of the two-body interaction are also the same as used by Sharma *et al* [16]. The relative magnitudes of the parameters of the hexadecapole–hexadecapole parts of the two-body interaction were calculated from a relation suggested by Bohr and Mottelson [21]. According to them, the approximate magnitude of these coupling constants for isospin $T = 0$ is given by

$$\chi_\lambda = \frac{4\pi}{2\lambda+1}\frac{m\omega_0^2}{A\langle r^{2\lambda-2}\rangle} \quad \text{for } \lambda = 1, 2, 3, 4 \tag{1}$$

and the parameters for $T = 1$ are approximately half the magnitude of their $T = 0$ counterparts. This relation was used to calculate the values of $\chi_{\rm pp4}$ relative to $\chi_{\rm pp}$ by generating the wave function for strontium isotopes and then calculating the values of $\langle r^{2\lambda-2}\rangle$ for $\lambda = 2$ and 4.

The values for hexadecapole–hexadecapole part of the two-body interaction turn out to be

$$\chi_{\rm pp4}(=\chi_{\rm nn4}) = -0.00033 \text{ MeV b}^{-8} \quad \text{and} \quad \chi_{\rm pn4} = -0.00066 \text{ MeV b}^{-8}.$$

2.2 *Projection of states of good angular momentum from axially-symmetric HB intrinsic states*

The procedure for obtaining the axially symmetric HB intrinsic states has been discussed in ref. [22].

2.3 *The variation-after-angular-momentum projection (VAP) method*

The VAP calculations have been carried out as follows: We first generated the self-consistent HB solutions, $\Phi(\beta)$, by carrying out the HB calculations with the Hamiltonian $(H - \beta Q_0^2)$, where β is a variational parameter. The selection of the optimum intrinsic states, $\Phi_{\rm opt}(\beta_J)$, is then made by finding out the minimum of the projected energy

$$E_J(\beta) = \langle\Phi(\beta)|HP^J_{00}|\Phi(\beta)\rangle/\langle\Phi(\beta)|P^J_{00}|\Phi(\beta)\rangle \tag{3}$$

as a function of β. In other words, the optimum intrinsic state for each yrast J satisfies the condition

$$\partial/\partial\beta[\langle\Phi(\beta)|HP^J_{00}|\Phi(\beta)\rangle/\langle\Phi(\beta)|P^J_{00}|\Phi(\beta)\rangle]|_{\beta=\beta_J} = 0. \tag{4}$$

3. Deformation systematics of Sr isotopes

From the systematics of 2^+ states in $^{98-102}$Sr, it is observed that the energy of 2^+ states decreases from 0.144 MeV in ^{98}Sr to 0.129 MeV in ^{100}Sr giving an indication that there is an increase in the degree of deformation as we move from ^{98}Sr to ^{100}Sr. This fact is also confirmed by the increase in the ratio E_4^+/E_2^+. The value of this ratio for ^{98}Sr is 3.00 whereas its value for ^{100}Sr is 3.23. For a rotational nucleus, the value of this ratio is 3.33. Besides this, it is observed that the 2^+ state does not change much as we move from ^{100}Sr to ^{102}Sr and it changes only marginally by a factor of 0.003 MeV. This is indicative of the fact that if asymptotic deformation has taken place in ^{102}Sr, there is very little chance of increasing deformation thereafter. This fact is also indicated by a small change in the value of the ratio E_4^+/E_2^+ from ^{100}Sr to ^{102}Sr. The value of this ratio changes from 3.23 for ^{100}Sr to the recently predicted value of 3.31 for ^{102}Sr [11]. Phenomenologically, it is well known that a nucleus having a smaller value of 2^+ energy should have a larger deformation. Since Q_2^+ of a nucleus is directly related to its intrinsic quadrupole moment, one should, therefore, expect that a smaller energy value for 2^+ state should manifest itself in terms of a larger value for the ratio of intrinsic quadrupole moment to the maximum possible intrinsic quadrupole moment for that nucleus in the $SU(3)$ limit $(\langle Q_0^2\rangle_{\rm HB}/\langle Q_0^2\rangle_{\rm max})$ denoted hereafter as RQ and vice versa. (The $SU(3)$ limit of the quadrupole moment for a particular nucleus in the HB framework is calculated by putting all the SPEs of the valence orbits equal to zero and thereby allowing the Nilsson orbits to fill up in the increasing order of quadrupole moment.) In other words, the observed systematics of E_2^+ with A should produce a corresponding

Table 1. The experimental values of excitation energy of the E_2^+ state in MeV, proton ($\langle Q_0^2\rangle_\pi$) and neutron ($\langle Q_0^2\rangle_\nu$) intrinsic quadrupole moments, ratio (RQ) of intrinsic quadrupole moment ($\langle Q_0^2\rangle_{\rm HB}$) to the maximum possible value ($\langle Q_0^2\rangle_{\rm max}$) and the ratio E_4^+/E_2^+ for $^{98-106}$Sr isotopes obtained with PQH interaction. The quadrupole moments have been computed in units of b^2, where $b = \sqrt{\hbar/m\omega}$ is the oscillator parameter.

Sr nuclei (A)	E_2^+ (exp.)*	$\langle Q_0^2\rangle_\pi$	$\langle Q_0^2\rangle_\nu$	$\langle Q_0^2\rangle_{\rm HB}$	$\langle Q_0^2\rangle_{\rm max}$	RQ	E_4^+/E_2^+ (exp.)
98	0.144	35.18	36.44	71.62	118.10	0.60	3.00*
100	0.129	35.55	38.17	73.72	115.17	0.64	3.23*
102	0.126	35.47	38.83	74.30	110.04	0.67	3.31**
104	–	35.19	39.26	74.45	104.19	0.71	–
106	–	34.85	39.86	74.71	98.17	0.76	–

*Data taken from refs [7–10,31,32].

**Data taken from ref. [11].

inverse systematics of this ratio of quadrupole moments for the $^{98-106}$Sr with increasing A. Based on the above logic, the calculated values of this ratio of intrinsic quadrupole moment should therefore exhibit an increase in its value as we move from ^{98}Sr to ^{102}Sr and thereafter, it should show very small increase which could be indicative of the asymptotic onset of deformation in heavy Sr isotopes. In table 1, the results of HB calculations are presented. Note that the ratio RQ increases from 0.60 to 0.76 as we move from ^{98}Sr to ^{106}Sr.

We next focus our attention on the factors that could be responsible for the deformation of neutron-rich Sr isotopes. In this regard, it is important to discuss and highlight some of the well-accepted factors responsible for bringing sizeable collectivity in nuclei in the same mass region. It is generally felt that the neutron–proton (np) effective interactions possess a deformation producing tendency and the neutron–neutron (nn) or proton–proton (pp) effective interactions are mostly of spherifying nature [23–28]. These ideas have played a pivotal role in the development of the stretch scheme [26] of Danos and Gillet, the rotor model [27] of Arima and Gillet and the interacting boson model of Arima *et al* [28]. In this regard, the role of np interaction in spin-orbit partner (SOP) orbits in the context of general development of collective features was also suggested by Federman and Pittel [23] and Casten *et al* [29]. Their calculations provided evidence suggesting that np interaction between the valence nucleons in the SOP orbits – the orbits $(g_{9/2})_\pi$ and $(g_{7/2})_\nu$ – may be instrumental *vis-à-vis* the observed onset of deformation in Sr isotopes with $A \geq 100$. It may also be pointed out that the role of np interaction between the SOP orbits in producing deformation depends critically on the relative occupation probability of $(g_{9/2})_\pi$ and $(g_{7/2})_\nu$ orbits [30].

As is evident from the results presented in table 1, the deformation appearing in heavy Sr isotopes is 60% in ^{98}Sr and 76% in ^{106}Sr of the maximum possible deformation in these isotopes. This is indicated by the fact that RQ values change from 0.60 to 0.76 as we move from ^{98}Sr to ^{106}Sr. In order to understand how

Table 2. The subshell occupation numbers (protons) in the $^{98-106}$Sr nuclei with PQH interaction.

Sr nuclei	Subshell occupation number								
(A)	$3s_{1/2}$	$2p_{1/2}$	$2p_{3/2}$	$2d_{3/2}$	$2d_{5/2}$	$1f_{5/2}$	$1g_{7/2}$	$1g_{9/2}$	$1h_{11/2}$
98	0.10	0.55	2.26	0.06	0.68	3.17	0.04	3.09	0.00
100	0.11	0.58	2.24	0.06	0.75	3.18	0.04	3.03	0.00
102	0.10	0.59	2.22	0.05	0.76	3.17	0.03	3.03	0.00
104	0.08	0.61	2.22	0.03	0.77	3.17	0.03	3.07	0.00
106	0.06	0.63	2.21	0.02	0.76	3.16	0.02	3.12	0.00

Table 3. The subshell occupation numbers (neutrons) in the $^{98-106}$Sr nuclei with PQH interaction.

Sr nuclei	Subshell occupation number								
(A)	$3s_{1/2}$	$2p_{1/2}$	$2p_{3/2}$	$2d_{3/2}$	$2d_{5/2}$	$1f_{5/2}$	$1g_{7/2}$	$1g_{9/2}$	$1h_{11/2}$
98	0.73	1.99	3.98	1.32	3.04	5.97	2.21	9.80	2.92
100	0.82	1.99	3.98	1.43	3.05	5.97	2.76	9.81	3.70
102	0.94	1.99	3.98	1.55	4.01	5.97	3.27	9.84	4.40
104	1.06	1.99	3.98	1.68	4.49	5.99	3.78	9.88	5.14
106	1.14	1.99	3.99	1.79	4.84	5.99	4.24	9.92	6.10

this deformation arises, we present in tables 2 and 3, the results of occupation probabilities of various proton and neutron subshells. These results have been obtained using PQH interaction.

From table 2, it is observed that $p_{1/2}$, $p_{3/2}$, $f_{5/2}$ proton subshells are partially filled. The polarization of these subshells could be one of the important factors contributing to the appearance of deformation in Sr isotopes. Secondly, it is observed from this table that $(g_{9/2})_\pi$ occupation is sizeable and from table 3, one notices that there are neutrons in $g_{7/2}$ subshell. Thus, there is an opportunity for neutron–proton (np) interaction in spin-orbit partner (SOP) orbits – the orbits $(g_{9/2})_\pi$ and $(g_{7/2})_\nu$ – in this case, to operate. As pointed out by Federman and Pittel [13,23], this factor could also lead to deformation in heavy Sr isotopes. From table 3, we also notice that low k-components of $(h_{11/2})_\nu$ orbits are occupied in ^{98}Sr to ^{106}Sr. Since these low k-components are sharply downsloping, their occupation could also lead to large deformation in these isotopes. This has been claimed to be the mechanism behind large onset of deformation in Sr isotopes by mean field theorists [14,15]. From the above discussion, it is evident that there are three factors responsible for the deformation in ^{98}Sr to ^{106}Sr. The first factor is the polarization of $2p_{1/2}$, $2p_{3/2}$ and $2f_{5/2}$ proton subshells. Because of this polarization, the protons tend to occupy $1g_{9/2}$ proton orbit which makes it possible for np interaction to operate between SOP orbits – the $(g_{9/2})\pi$ and $(g_{7/2})\nu$ orbits in the present context – as

there are already neutrons in $(g_{7/2})$ orbit. Besides this, the increasing trend in the occupation probability of $(1h_{11/2})\nu$ reinforces the development of deformation as we move from ^{98}Sr to ^{106}Sr. It may be noted that $(h_{11/2})\nu$ orbit is nearly half-filled in ^{106}Sr making maximum contribution to the quadrupole moment.

4. Energy spectra in $^{98-106}$Sr

Now to test the reliability and efficiency of HB calculations performed with PQH model of two-body interaction, it is important to obtain satisfactory agreement for the yrast spectra. A projection calculation for the energy spectra of $^{98-106}$Sr has been carried out by employing the phenomenological PQ and PQH models of two-body interaction in the following manner:

Starting from the Hamiltonian $(H - \beta Q_0^2)$, HB intrinsic state was obtained for a number of values of variational parameter (β) for each Sr isotope. From these intrinsic states, even spin and even parity angular momentum states were projected out. Then, the lowest energy value (E_J^+) corresponding to each angular momentum state (J^+) is collected to obtain the yrast spectra in each Sr nucleus.

In figures 1a and 1b, the yrast spectra for $^{98-106}$Sr is displayed. The spectra corresponding to Th.1 is obtained when PQ model of interaction is employed, whereas the spectra corresponding to Th.2 is obtained when PQH model of interaction is employed. It may be noted that the spectra corresponding to Th.2 is in satisfactory agreement with the experiment [31,32] and there is lot of improvement as we go from the spectra corresponding to Th.1 to the spectra corresponding to Th.2 when compared with the observed spectra. For example, in the case of ^{98}Sr, the observed yrast 8^+, 10^+ and 12^+ energy states are having energies 1.43 MeV, 2.12 MeV and 2.93 MeV respectively and the Th.1 spectra give the corresponding energy values as 3.30 MeV, 4.90 MeV and 6.80 MeV, which are sharply in disagreement with the observed yrast states. However, the projection calculations presented under Th.2 spectra give the energy values as 1.30 MeV, 2.00 MeV and 2.80 MeV for the yrast 8^+, 10^+ and 12^+ states respectively. It is, therefore, very obvious that the energy values calculated under Th.2 are in satisfactory agreement with the observed energy values. The same trend is also observed for ^{100}Sr isotope. We can, therefore, make a comment that the study of yrast spectra in $^{98-100}$Sr indicates that PQH model of interaction is an improvement over the PQ model of interaction in the case of Sr isotopes. Since the experimental spectra for $^{102-106}$Sr is not available (only upto 2^+ state in ^{102}Sr is available), it turns out that the different yrast states predicted by the Th.2 calculations for ^{102}Sr, ^{104}Sr and ^{106}Sr will serve as a motivation for the experimentalists to look for these states in $^{102-106}$Sr. It may be noted that the calculations of spectra are carried out for the entire set of the $^{98-106}$Sr isotopes with a single set of input parameters. In table 4, the values of the variational parameter (β), corresponding to which the yrast spectra for Th.2 has been obtained, are presented.

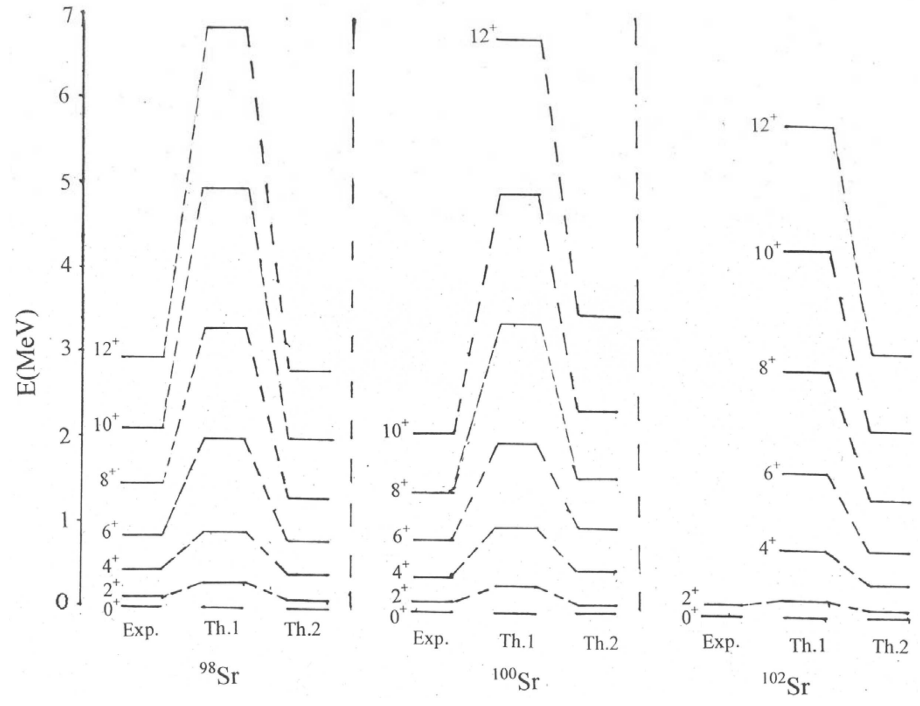

(a)

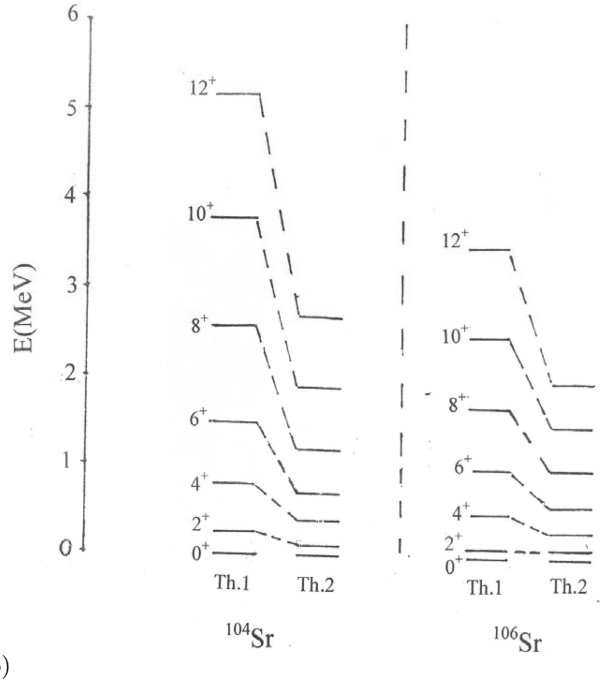

(b)

Figure 1. (**a**) Experimental and theoretical low-lying yrast spectra for $^{98-102}$Sr nuclei. (**b**) Theoretical low-lying yrast spectra for $^{104-106}$Sr nuclei.

Table 4. Values of the variational parameter (β) and spins (I^+) corresponding to which the yrast spectra for Th.2 has been obtained in $^{98-106}$Sr.

Nucleus	Spins (I^+)	Variational parameter (β)
^{98}Sr	$0^+ \rightarrow 6^+$	0.0
	$8^+ \rightarrow 10^+$	0.15
	$12^+ \rightarrow 16^+$	0.20
^{100}Sr	$0^+ \rightarrow 8^+$	0.0
	$10^+ \rightarrow 12^+$	0.10
	$14^+ \rightarrow 16^+$	0.15
^{102}Sr	$0^+ \rightarrow 8^+$	0.0
	$10^+ \rightarrow 14^+$	0.15
	16^+	0.20
^{104}Sr	$0^+ \rightarrow 4^+$	0.0
	$6^+ \rightarrow 12^+$	0.10
	$14^+ \rightarrow 16^+$	0.15
^{106}Sr	$0^+ \rightarrow 8^+$	0.0
	$10^+ \rightarrow 12^+$	0.10
	$14^+ \rightarrow 16^+$	0.15

5. Systematics of the calculated values of $E2$ transition probabilities in Sr isotopes

The reliability and goodness of the HB wave function is also examined by calculating the $B(E2)$ values. In table 5, the calculated values of $E2$ transition probabilities between the states E_J and E_{J+2} are presented. The calculated values are expressed in parametric form in terms of the proton ($e_{\rm p}$) and neutron ($e_{\rm n}$) effective charges, such that $e_{\rm p} = 1 + e_{\rm eff}$ and $e_{\rm n} = e_{\rm eff}$, and have been obtained through a rigorous projection calculation. The $B(E2{:}\ J_i^+ \rightarrow J_f^+)$ values have been calculated in units of $\mathrm{e}^2\mathrm{b}_{\rm n}^2$ (where $\mathrm{b}_{\rm n}$ stands for barn, 1 barn $= 10^{-28}$ m^2). The results indicate that by choosing $e_{\rm eff} = 0.25$, a good agreement with the observed values for $B(E2{:}\ 0^+ \rightarrow 2^+)$ transition probabilities is obtained for $^{98-100}$Sr nuclei. For example, in ^{98}Sr, the calculated value of $B(E2{:}\ 0^+ \rightarrow 2^+)$ is 1.41 units and experimental value is 1.28(39) units. Similarly for ^{100}Sr, the calculated and observed values of $B(E2{:}\ 0^+ \rightarrow 2^+)$ are 1.34 units and 1.42(8) units respectively. The experimental data for the higher transitions in $^{98-100}$Sr is not available but we have calculated the data for the higher transitions, upto $8^+ \rightarrow 10^+$, also. Similarly, the experimental data for any of the transitions in $^{102-106}$Sr is not available but we have also calculated the data upto $8^+ \rightarrow 10^+$ transitions, corresponding to the same effective charge as used for ^{98,100}Sr, in these nuclei.

From the comparison of the calculated $B(E2)$ values with the experimental values [34] for the $0^+ \rightarrow 2^+$ transitions in $^{98-100}$Sr, it is satisfactory to note that the calculated $B(E2)$ values are in good agreement with the experiments. Since the

Table 5. The reduced transition probabilities for $E2$ transitions for the yarst levels in the nuclei $^{98-106}$Sr. Here $e_{\rm p}(e_{\rm n})$ denotes the effective charge for protons (neutrons). The entries presented in the third column correspond to the reduced matrix elements of the quadrupole operator between yrast states [16]. The reduced matrix elements have been expressed in a form that brings out their explicit dependence on the effective charges. The entries presented in the fourth column correspond to the effective charges indicated in the first column. The $B(E2)$ values are in units of $\mathrm{e}^2\mathrm{b}_{\rm n}^2$ (where $\mathrm{b}_{\rm n}$ stands for barn, 1 barn = 10^{-28} m^2).

Nucleus	Transition		$B(E2\colon J_i^+ \to J_f^+)$	
$(e_{\rm p}, e_{\rm n})$	$(J_i^+ \to J_f^+)$	$[B(E2\colon J_i^+ \to J_f^+)]^{1/2}_{\rm th}$	Theory	(Exp.)*
(1)	(2)	(3)	(4)	(5)
^{98}Sr (1.25, 0.25)	$0^+ \to 2^+$	$0.75e_{\rm p}+1.00e_{\rm n}$	1.41	1.28(39)
	$2^+ \to 4^+$	$0.90e_{\rm p}+1.19e_{\rm n}$	2.02	–
	$4^+ \to 6^+$	$0.94e_{\rm p}+1.25e_{\rm n}$	2.21	–
	$6^+ \to 8^+$	$0.95e_{\rm p}+1.28e_{\rm n}$	2.27	–
	$8^+ \to 10^+$	$0.95e_{\rm p}+1.30e_{\rm n}$	2.28	–
^{100}Sr (1.25, 0.25)	$0^+ \to 2^+$	$0.76e_{\rm p}+0.84e_{\rm n}$	1.34	1.42(8)
	$2^+ \to 4^+$	$0.91e_{\rm p}+0.93e_{\rm n}$	1.87	–
	$4^+ \to 6^+$	$0.95e_{\rm p}+0.98e_{\rm n}$	2.05	–
	$6^+ \to 8^+$	$0.97e_{\rm p}+1.00e_{\rm n}$	2.13	–
	$8^+ \to 10^+$	$0.98e_{\rm p}+1.01e_{\rm n}$	2.18	–
^{102}Sr (1.25, 0.25)	$0^+ \to 2^+$	$0.78e_{\rm p}+0.68e_{\rm n}$	1.31	–
	$2^+ \to 4^+$	$0.93e_{\rm p}+0.81e_{\rm n}$	1.86	–
	$4^+ \to 6^+$	$0.97e_{\rm p}+0.86e_{\rm n}$	2.03	–
	$6^+ \to 8^+$	$0.99e_{\rm p}+0.88e_{\rm n}$	2.12	–
	$8^+ \to 10^+$	$0.99e_{\rm p}+0.90e_{\rm n}$	2.13	–
^{104}Sr (1.25, 0.25)	$0^+ \to 2^+$	$0.78e_{\rm p}+0.91e_{\rm n}$	1.44	–
	$2^+ \to 4^+$	$0.93e_{\rm p}+1.08e_{\rm n}$	2.05	–
	$4^+ \to 6^+$	$0.98e_{\rm p}+1.13e_{\rm n}$	2.27	–
	$6^+ \to 8^+$	$0.99e_{\rm p}+1.16e_{\rm n}$	2.33	–
	$8^+ \to 10^+$	$0.99e_{\rm p}+1.17e_{\rm n}$	2.34	–
^{106}Sr (1.25, 0.25)	$0^+ \to 2^+$	$0.78e_{\rm p}+0.69e_{\rm n}$	1.31	–
	$2^+ \to 4^+$	$0.93e_{\rm p}+0.83e_{\rm n}$	1.87	–
	$4^+ \to 6^+$	$0.97e_{\rm p}+0.87e_{\rm n}$	2.04	–
	$6^+ \to 8^+$	$0.99e_{\rm p}+0.89e_{\rm n}$	2.13	–
	$8^+ \to 10^+$	$1.00e_{\rm p}+0.91e_{\rm n}$	2.18	–

*Exp. data taken from ref. [34].

experimental data for the higher transitions in $^{98-100}$Sr and any of the transitions in $^{102-106}$Sr are not available, it turns out that the calculated data predicted for different transitions in $^{98-106}$Sr will serve as a motivation for the experimentalists to look for this data.

6. Quadrupole deformations (β_2) in Sr isotopes

We have calculated values for deformation parameter (β_2) for $^{98-106}$Sr. The deformation parameter β_2 is related to $B(E2)\uparrow$ by the formula suggested by Raman *et al* [33] as

$$\beta_2 = (4\pi/3ZR_0^2)[B(E2)\uparrow/e^2]^{1/2}, \tag{5}$$

where R_0 is usually taken to be 1.2 $A^{1/3}$ fm and $B(E2)\uparrow$ is in units of $e^2b_n^2$.

The deformation parameter β_2 has been calculated using the calculated $B(E2)\uparrow$ values, given in table 5. From the calculations, we find that β_2 values for the nuclei ^{98}Sr, ^{100}Sr, ^{102}Sr, ^{104}Sr and ^{106}Sr are 0.42, 0.41, 0.40, 0.41 and 0.39 respectively. The experimental values [34] for ^{98}Sr and ^{100}Sr are 0.40(6) and 0.42(12) respectively. From the comparison of the data, we find that there is reasonable agreement for β_2 values for the nuclei $^{98-100}$Sr. The experimental data for $^{102-106}$Sr are not available.

7. Conclusions

From the results of our calculations, the following conclusions can be drawn:

(i) The VAP calculations performed with PQH interaction reproduce correctly the observed deformation systematics in $^{98-102}$Sr isotopes. The deformation develops because of the simultaneous polarization of $(p_{3/2})$ and $(f_{5/2})$ proton subshells and the operation of np interaction between $(g_{9/2})_\pi$ and $(g_{7/2})_\nu$ subshells. The polarization of $p_{3/2}$ or $f_{5/2}$ orbits is an important pre-requisite for the np interaction between SOP orbits to operate.

(ii) The yrast spectra obtained with the inclusion of hexadecapole interaction shows satisfactory agreement with the observed spectra compared to the spectra obtained with PQ model of interaction.

(iii) The values of hexadecapole interaction parameters employed by us are the appropriate ones in this mass region as, with them, the HB wave function yields values of $B(E2)$ which are in satisfactory agreement with experiments.

References

[1] E Cheifetz, R C Jarad, S G Thompson and J B Wilhelmy, *Phys. Rev. Lett.* **25,** 38 (1970)

[2] H Ohm, G Lhersonneau, K Sistemich, B Pfeiffer and K L Kratz, *Z. Phys.* **A327**, 483 (1987)

[3] G Lhersonneau, H Gabelmann, K L Kratz, B Pfeiffer, N Kaffrell and the ISOLDE Collaboration, *Z. Phys.* **A332**, 243 (1989)

[4] G Lhersonneau, H Gabelmann, N Kaffrell, K L Kratz, B Pfeiffer, K Heyde and the ISOLDE Collaboration, *Z. Phys.* **A337**, 143 (1990)

[5] F Buchinger, E B Ramsay, E Arnold, W Neu, R Neugart, K Wendt, R Silverans, E Lievens, L Vermeeren, D Berdichevsky, R Fleming and D W L Sprung, *Phys. Rev.* **C41**, 2883 (1990)

[6] P Lievens, R E Silverans, L Vermeeren, W Borchers, W Neu, R Neugart, K Wendt, F Buchinger, E Arnold and the ISOLDE Collaboration, *Phys. Lett.* **B256**, 141 (1991)
[7] G Lhersonneau, B Pfeiffer, R Capote, J M Quesada, H Gabelmann, K L Kratz and the ISOLDE Collaboration, *Phys. Rev.* **C65**, 024318 (2002)
[8] R E Azuma, G L Borchert, L C Carraz, P G Hansen, B Jonson, S Matttsson, O B Nielsen, G Nyman, I Ragnarson and H L Ravn, *Phys. Lett.* **B86**, 5 (1979)
[9] J H Hamilton, A V Ramayya, S J Zhu, G M Ter-Akopia, Yu Oganessian, J D Cole, J O Rasmussen and M A Stoyer, *Prog. Part. Nucl. Phys.* **35**, 635 (1995)
[10] G Lhersonneau, B Pfeiffer, M Huhta, A Wohr, I Klockl, K L Gratz, J Aysto and the ISOLDE Collaboration, *Z. Phys.* **A351**, 357 (1995)
[11] S Verma, P Ahmad, R Devi and S K Khosa, *Phys. Rev.* **C77**, 024308 (2008)
[12] John C Hill, J A Winger, F K Wohn, R F Petry, J D Goulden, R L Gill, A Piotrowski and H Mach, *Phys. Rev.* **C33**, 5 (1985)
[13] P Federman and S Pittel, *Phys. Rev.* **C20**, 820 (1979)
[14] P Bonche, H Flocard, P H Heenen, S J Krieger and M S Weiss, *Nucl. Phys.* **A443**, 39 (1985)
[15] X Campi and M Epherre, *Phys. Rev.* **C22**, 2605 (1980)
[16] S K Sharma, P N Tripathi and S K Khosa, *Phys. Rev.* **C38**, 2935 (1988)
[17] P N Tripathi, S K Sharma and S K Khosa, *Phys. Rev.* **C29**, 1951 (1984)
[18] S K Khosa, P N Tripathi and S K Sharma, *Phys. Lett.* **B119**, 257 (1982)
[19] S K Khosa and S K Sharma, *Phys. Rev.* **C25**, 2715 (1981)
[20] J D Vergados and T T S Kuo, *Phys. Lett.* **B35**, 93 (1971)
[21] A Bohr and B R Mottelson, *Nuclear structure* (Benjamin, New York, 1975) Vol. II, p. 356
[22] S K Sharma, *Nucl. Phys.* **A260**, 226 (1976)
[23] P Federman and S Pittel, *Phys. Lett.* **B69**, 385 (1977)
[24] S Pittel, *Nucl. Phys.* **A347**, 417 (1980)
[25] S C K Nair, A Ansari and L Satpathi, *Phys. Lett.* **B71**, 257 (1977)
[26] M Danos and V Gillet, *Phys. Rev.* **C161**, 1034 (1967)
[27] A Arima and V Gillet, *Ann. Phys.* **66**, 117 (1971)
[28] A Arima, T Ohtsuka, F Lachella and I Talmi, *Phys. Lett.* **B66**, 205 (1977)
[29] R F Casten *et al*, *Phys. Lett.* **47**, 1433 (1981)
[30] P K Mattu and S K Khosa, *Phys. Rev.* **C39**, 2018 (1989)
[31] M Sakai, *At. Data Nucl. Data Tables* **31**, 409 (1984)
[32] B Singh and Z Hu, *Nucl. Data Sheets* **98**, 335 (2003)
[33] S Raman, C W Nestor, S Kahane and K H Bhatt, *At. Data Nucl. Data Tables* **42**, 1 (1989)
[34] S Raman, C W Nestor and P Tikkanen, *At. Data Nucl. Data Tables* **78**, 40 (2001)